TM No. 85-1045
cy 001

NAVAL UNDERWATER SYSTEMS CENTER
NEW LONDON LABORATORY
NEW LONDON, CONNECTICUT 06320

Technical Memorandum

ON THE IMPEDANCE OF A LOSSY TRANSDUCER

Date: 22 March 1985

Prepared by: Mark B Moffett
MARK B. MOFFETT
Surface Ship
Sonar Department

Report Documentation Page

Form Approved
OMB No. 0704-0188

1. REPORT DATE	2. REPORT TYPE	3. DATES COVERED
22 MAR 1985	**Technical Memo**	**22-03-1985 to 22-03-1985**

4. TITLE AND SUBTITLE
On the Impedance of a Lossy Transducer

5a. CONTRACT NUMBER

5b. GRANT NUMBER

5c. PROGRAM ELEMENT NUMBER

6. AUTHOR(S)
Mark Moffett

5d. PROJECT NUMBER
A65250

5e. TASK NUMBER

5f. WORK UNIT NUMBER

7. PERFORMING ORGANIZATION NAME(S) AND ADDRESS(ES)
Naval Underwater Systems Center,New London,CT,06320

8. PERFORMING ORGANIZATION REPORT NUMBER
TM No. 851045

9. SPONSORING/MONITORING AGENCY NAME(S) AND ADDRESS(ES)
ONR Code 220

10. SPONSOR/MONITOR'S ACRONYM(S)

11. SPONSOR/MONITOR'S REPORT NUMBER(S)

12. DISTRIBUTION/AVAILABILITY STATEMENT
Approved for public release; distribution unlimited

13. SUPPLEMENTARY NOTES
NUWC2015

14. ABSTRACT

Many transducer materials exhibit negligible dielectric losses and are represented by models or equivalent circuits containing only mechanical loss mechanisms. In contrast however, polymer hydrophone materials are known to exhibit appreciable dielectric losses at high frequencies. In order to elucidate the effects of dielectric losses, a simple equivalent circuit containing a lossy clamped capacitance is analyzed. Plots of the electrical input impedance are presented for various electrical and mechanical quality factors and for various values of the coupling coefficient. A method for determining the frequencies of maximum and minimum impedance is derived.

15. SUBJECT TERMS
transducers; dielectric losses; polymer hydrophone materials

16. SECURITY CLASSIFICATION OF:			17. LIMITATION OF ABSTRACT	18. NUMBER OF PAGES	19a. NAME OF RESPONSIBLE PERSON
a. REPORT	b. ABSTRACT	c. THIS PAGE			
unclassified	**unclassified**	**unclassified**	**Same as Report (SAR)**	**28**	

ABSTRACT

Many transducer materials exhibit negligible dielectric losses and are represented by models or equivalent circuits containing only mechanical loss mechanisms. In contrast, however, polymer hydrophone materials are known to exhibit appreciable dielectric losses at high frequencies. In order to illucidate the effects of dielectric losses, a simple equivalent circuit containing a lossy clamped capacitance is analyzed. Plots of the electrical input impedance are presented for various electrical and mechanical quality factors and for various values of the coupling coefficient. A method for determining the frequencies of maximum and minimum impedance is derived.

ADMINISTRATIVE INFORMATION

This memorandum was prepared under Job Order No. A65250, "Extended Sensor Modelling," Principal Investigator: B. E. McTaggert, Code 3234, Sponsoring Activity: ONR Code 220 (CAPT E. Craig). The author is located at the Naval Underwater Systems Center, New London, CT 06320.

I. INTRODUCTION

Losses in piezoelectric transducers are often considered to be strictly mechanical, rather than electrical, in nature. This view may be justified in many cases, but Martin[1] has pointed out that dielectric and piezoelectric losses must also be included in an adequate transducer description. Morever, measurements[2] of the permittivity of polyvinylidene fluoride (PVDF), a polymer piezoelectric material, indicate that the dielectric loss factor can be as high as 0.3 for nonvoided PVDF at high frequencies ($\geq$1 MHz). It seems possible that some flexible composite piezoelectric materials may also have appreciable dielectric losses, since the polymer matrix is sometimes blended with carbon to increase the electrical conductivity and reduce the required electric poling field.[3] At any rate, a look at the implications of finite electrical losses for piezoelectric transducers appears to be in order.

II. EQUIVALENT CIRCUIT

The equivalent circuit for a piezoelectric resonator[4] includes a mechanical transmission line in order to account for wave effects, such as the standing wave which occurs when the element is one-half wavelength long. In our discussion of dielectric losses, we wish to focus on the behavior near that half-wavelength condition, and so we can use the simplified equivalent circuit, valid near resonance, of Figure 1. In the figure, C_o is the clamped electrical capacitance of the element, k is the appropriate coupling constant, ω_s is the series resonance (angular) frequency of the mechanical branch, and Q_e and Q_m are the electrical and mechanical quality factors, respectively. Parallel resonance (antiresonance) of the electrical and mechanical branches occurs at

$$\omega_p = \sqrt{1 + 8(k/\pi)^2}\ \omega_s \qquad (1)$$

The circuit of Figure 1 is valid as long as $k^2 << 1$; otherwise, the frequency band covering ω_s and ω_p becomes too large to be fairly represented by a lumped-element circuit.

If we consider the piezoelectric resonator as a bar or plate having dimensions ℓ_1, ℓ_2, and ℓ_3, respectively, along the x_1, x_2, and x_3 axes of the piezoelectric material, the circuit parameters are related to the material properties as follows:[4]

1) Thickness plate resonator:

$$k^2 = h_{33}^2 \epsilon_{33}^S / c_{33}^D \quad , \tag{2}$$

$$C_0 = \epsilon_{33}^S \ell_1 \ell_2 / \ell_3 \quad , \tag{3}$$

$$\omega_p = \pi v_t^D / \ell_3 \quad , \tag{4}$$

$$v_t^D = \left(c_{33}^D / \rho \right)^{1/2} \quad , \tag{5}$$

where h_{33} is the piezoelectric strain and charge density constant, ϵ_{33}^S the clamped permittivity, c_{33}^D the open circuit stiffness in the poled direction, v_t^D, the open circuit thickness wave velocity, and the density. As given by Equation 2, k is the thickness coupling factor.

2) 33 bar resonator:

$$k^2 = k_{33}^2 = d_{33}^2 / \epsilon_{33}^T s_{33}^E \quad , \tag{6}$$

$$C_0 = \epsilon_{33}^T (1 - k^2) \ell_1 \ell_2 / \ell_3 \quad , \tag{7}$$

$$\omega_p = \pi v_b^D / \ell_3 \quad , \tag{8}$$

$$v_b^D = [\rho s_{33}^E (1-k^2)]^{-1/2} \tag{9}$$

where k_{33} is the 33 coupling factor, d_{33} the piezoelectric stress and electric field constant, ε_{33}^T the free permittivity, s_{33}^E, the short circuit compliance (in the poled direction), and V_b^D the open circuit extensional wave velocity in the poled direction.

3) 31 bar resonator:

$$k^2 = k_{31}^2 = d_{31}^2 / \epsilon_{33}^T s_{11}^E \quad , \tag{10}$$

$$C_o = \epsilon_{33}^T (1-k^2) \ell_1 \ell_2 / \ell_3 \quad , \tag{11}$$

$$\omega_s = \pi v_b^E / \ell_3 \quad , \tag{12}$$

$$v_b^E = (\rho s_{11}^E)^{-1/2} \quad , \tag{13}$$

where k_{31} is the 31 coupling factor, d_{31} the piezoelectric stress and electric field constant, s_{11}^E the short circuit compliance (in the stretched direction), and V_b^E the short circuit extensional wave velocity in the stretched (x_1) direction. Note that in the 31 case, the half-wave condition occurs at the series resonance frequency, ω_s, where the electrical input impedance is small, whereas in the 33 and thickness modes, the half-wave condition occurs at the parallel resonance, ω_p, where the impedance is large.

Electrical and mechanical losses have been introduced into the equivalent circuit of Figure 1 through the use of the quality factors, Q_e and Q_m. (Q_e is the reciprocal of the dielectric dissipation factor.) Although, for our discussion, these quality factors will be assumed independent of frequency, a better representation of the losses would allow the quality factors to vary with frequency. We have chosen the resistances of Figure 1 to vary with frequency in the same way as their corresponding reactive components, i.e, proportional to ωL for the mechanical loss resistance and inversely proportional to ωC_o for the electrical loss resistance. We are thus assured that the series resistance will never exceed the reactance, ωL, and that the parallel resistance will always exceed the reactance, $1/\omega C_o$.

III. IMPEDANCE PLOTS

The square of the magnitude of the normalized impedance, $\omega_s C_o Z$, of the equivalent circuit of Figure 1 is

$$\left|\omega_s C_o Z\right|^2 = \frac{1}{\Omega} \frac{(\Omega-1)^2 + (\Omega/Q_m)^2}{[\Omega-(1+\gamma)]^2 + \left(\frac{\Omega-1}{Q_e}\right)^2 + \frac{\Omega}{Q_m}\left[\frac{\Omega}{Q_m}\left(1+\frac{1}{Q_e^2}\right)+\frac{2\gamma}{Q_e}\right]} \quad (14)$$

where $\Omega \triangleq (\omega/\omega_s)^2$ (15)

and $\gamma \triangleq 8(k/\pi)^2$. (16)

Figures 2 through 10 are plots of the normalized impedance magnitude, $|\omega_s C_o Z|$, as a function of the normalized frequency, ω/ω_s, for values of Q_e and Q_m of 100, 10, and 1. The three curves on each figure are for values of the coupling constant, k = 0.1, 0.2, and 0.5. At frequencies well removed from resonance, the impedance is that of a lossy capacitance. Referring to the circuit of Figure 1, we see that the low frequency (free) capacitance is $C_o + C = C_o (1 + \gamma)$ while the high frequency (clamped) value is C_o, but in each case, the shunt resistance is $Q\hat{e}/\omega C_o$. The offset between the high frequency asymptotic impedance and that at low frequencies is a measure of the coupling factor.[5] It can be obtained from Equation (14) as

$$\frac{\lim_{\omega \to \infty} |\omega Z|}{\lim_{\omega \to 0} |\omega Z|} = \left[\frac{(1+\gamma)^2 + Q_e^{-2}}{1 + Q_e^{-2}} \right]^{1/2} \qquad (17)$$

In the absence of electrical losses, the offset is $1 + \gamma$, the ratio of the free and clamped capacitances. When electrical losses are present, the offset is reduced as indicated by Equation (17). Mechanical losses have no effect on the offset ratio of Equation (17); their influence is felt only near resonance. The offset ratio is strongly dependent on the coupling factor, k, as can be seen in Equation (17) (the $1 + \gamma$ term) and in any of Figures 2-10.

We consider next the behavior of the impedance near resonance, where the influence of the mechanical branch of the equivalent circuit becomes important. Increases in either k or Q_m are well-known[6] to cause increases in the ratio of maximum and minimum impedance, $|Z_{max}|/|Z_{min}|$, as can be seen in Figures 2-10. The effect of finite electrical losses near resonance can be seen by comparison of Figures 2-4. Because the electrical loss is in a shunt element, it has a pronounced effect on the maximum

impedance $|Z_{max}|$, but very much less influence on $|Z_{min}|$, the minimum impedance, i.e., the loss resistance shunts out the high impedance, Z_{max}, but is itself shunted out by the low impedance, Z_{min}. Figures 5-7 and Figures 8-10 illustrate the same phenomenon for Q_m = 10 and 1, respectively. Electrical quality factors as low as 1 tend to pull the overall impedance level (i.e., over the whole frequency band) down because of this shunting action; compare, for example, Figures 3 and 4. Figure 11 is a plot of $|Z_{max}|/|Z_{min}|$ as a function of Q_e for various values of k and Q_m. As long as $Q_e \geq Q_m$, the effect of electrical losses is unimportant, but they become increasingly important as Q_e becomes less than Q_m, especially at the larger coupling factors.

IV. FREQUENCIES OF MAXIMUM AND MINIMUM IMPEDANCE

The frequencies, ω_{max} and ω_{min}, at which the impedance magnitude is maximum and minimum, respectively, can be found by differentiating Equation (14), i.e.,

$$d|\omega_s C_o Z|^2/d\Omega = 0 \tag{18}$$

Unfortunately, this process results in a quadratic equation in Ω, so that a direct solution for Ω_{max} and Ω_{min} is cumbersome. Equation (18) turns out to be only quadratic in γ, however, so that it is relatively easy to solve for γ in terms of Ω. In other words, we use Equation (18) to find values of γ that produce an impedance extremum at a given value of Ω. The resulting quadratic equation in γ is:

$$a\gamma^2 + b\gamma + c = 0, \tag{19}$$

where

$$a \equiv 1 - \left(1 + \frac{1}{Q_m^2}\right)\Omega^2 , \tag{20}$$

$$b \equiv 2\left[a + 2\left(1 - \frac{1}{Q_e Q_m}\right)\Omega(\Omega - 1)\right] \quad , \tag{21}$$

and $$c \equiv \left(1 + \frac{1}{Q_e^2}\right)\left[(\Omega - 1)^2 + (\Omega / Q_m)^2\right] . \tag{22}$$

The solutions for k are then

$$k_{\pm} = \pi \left(\gamma_{\pm} / 8\right)^{1/2} \quad , \tag{23}$$

where $$\gamma_{\pm} = \left[-b \pm (b^2 - 4ac)^{1/2}\right] / 2a . \tag{24}$$

Thus, for a given frequency ratio, ω/ω_s (recall $\Omega = (\omega/\omega_s)^2$), we found k_+ and k_-, corresponding to extrema of $|\omega_s C_o Z|$ at the given ω/ω_s. Figures 12 and 13 are plots of ω/ω_s versus k corresponding to these extrema for Q_m = 10 and 100, respectively. If k is very small, there are no extrema, but at some minimum value of k, the maximum and minimum impedances coincide, i.e., there is an inflection point, with zero slope, in the |Z| vs ω curve. At still larger values of k, Figures 12 and 13 show that there are two frequencies yielding extrema in |Z|. The lower frequency is the location of the impedance minimum and the higher one corresponds to the impedance maximum. In other words, the upper branch of each curve is ω_{max}/ω_s, while the lower branch is ω_{min}/ω_s. In the limit of very large Q_m and Q_e, the lower frequency becomes ω_s and the higher one is given by Equation (1); this situation is plotted in Figure 14. Comparison of Figures 12, 13, and 14 shows the effect of coupling and losses on ω_{max} and ω_{min}. Increasing k always increases the separation and the ratio betwen them, whereas decreases in either Q_e or Q_m result in an increase in $\omega_{max}/\omega_{min}$. These effects, (at least for infinite Q_e) have been illustrated in Figure 4 of Reference 7.

V. SUMMARY

The equivalent circuit of Figure 1 has provided us with an approximation to the effects of dielectric and mechanical losses in transducers, valid near resonance and for $k^2 << 1$. (A more precise treatment would involve an equivalent circuit containing a mechanical transmission line[4] and include piezoelectric losses[1] as well.) Finite electrical losses: 1) reduce the amount of offset between the high- and low-frequency asymptotes of $|Z|$ (see Equation (17)), 2) reduce the ratio $|Z_{max}|/|Z_{min}|$ (with a more pronounced effect on $|Z_{max}|$) (see Figure 11) and 3) increase the separation and ratio of ω_{max} and ω_{min} (see Figures 12 and 13).

VI. ACKNOWLEDGMENTS

The author thanks C. L. LeBlanc, H. B. Miller, and J. M. Powers, all of NUSC, and G. E. Martin, of Martin Acoustics Software Technology, for helpful discussions.

VII. REFERENCES

1. Gordon E. Martin, "Dielectric, elastic, and piezoelectric losses in piezoelectric materials," Proceedings of the 1974 IEEE Ultrasonics Symposium, pp. 613-617.

2. Mark B. Moffett and James M. Powers, "Dielectric properties of piezoelectric polyvinylidene fluoride (PVDF)," NUSC Technical Memorandum 841072, April 16, 1984.

3. R. E. Newnham, A. Safari, G. Sa-gong, and J. Giniewicz, "Flexible composite piezoelectric sensors," Proceedings of the 1984 IEEE Ultrasonics Symposium, pp. 501-506.

4. Don A. Berlincourt, Daniel R. Curran, and Hans Jaffe, "Piezoelectric and piezomagnetic materials and their function in transducers," in Physical Acoustics, Principles and Methods, Vol. IA, ed. by Warren P. Mason (Academic, New York, 1964), pp. 169-270.

5. Harry B. Miller, "Handbook for the analysis of piezolectric transducers, Part I: the untuned transducer," NUSC Technical Document 6029, Sept 14, 1978.

6. Kimio Shibayama, "Measurement of small values of electromechanical-coupling coefficient in piezoelectric transducers," J. Acoust. Soc. Am. 34, 1883-1886 (1962).

7. Gordon E. Martin, "Determination of equivalent-circuit constants of piezoelectric resonators of moderately low Q by absolute-admittance measurements," J. Acoust. Soc. Am. 26, 413-420 (1954).

VIII. GLOSSARY OF SYMBOLS

a	see Equation (20)
b	see Equation (21)
c	see Equation (22)
c_{33}^D	open circuit stiffness, x_3 - direction (Pa)
C	capacitance due to mechanical compliance, = γC_o (F)
C_o	clamped capacitance (F)
d_{31}	piezoelectric constant, 31 mode (C/N)
d_{33}	piezoelectric constant, 33 mode (C/N)
h_{33}	piezoelectric constant, thickness mode (V/m)
k	coupling factor, general
k_{31}	coupling factor, 31 mode, see Equation (10)
k_{33}	coupling factor, 33 mode, see Equation (6)
k_+, k_-	coupling factor roots of Equation (19)
ℓ_1	length of element, x_1 - direction (m)
ℓ_2	length of element, x_2 - direction (m)
ℓ_3	length of element, x_3 - direction (m)
L	inductance due to mass, = $(\omega_s^2 C)^{-1}$ (H)
Q_e	electrical quality factor, see Figure 1
Q_m	mechanical quality factor, see Figure 1
s_{11}^E	short-circuit compliance, x_1 - direction (Pa^{-1})
s_{33}^E	short-circuit compliance, x_2 - direction (Pa^{-1})
v_b^D	open-circuit bar-wave velocity, x_3 - direction (m/s)
v_b^E	short-circuit bar-wave velocity, x_1 - direction (m/s)
v_t^D	open-circuit thickness-wave velocity, x_3 - direction (m/s)
x_1	element crystal axis coordinate, stretch direction (m)
x_2	element crystal axis coordinate, (m)
x_3	element crystal axis coordinate, poled direction (m)
Z	(complex) electrical impedance (Ohms)
$\|Z\|$	absolute magnitude of Z (Ohms)
$\|Z_{max}\|$	maximum value of $\|Z\|$ (Ohms)

$\|Z_{min}\|$	minimum value of $\|Z\|$ (Ohms)
γ	$= 8\ (k/\pi)^2$
γ_+, γ_-	roots of Equation (19)
ε_{33}^S	clamped permittivity, x_3 - direction (F/m)
ε_{33}^T	free permittivity, x_3 - direction (F/m)
ρ	density (kg/m^3)
ω	angular frequency (rad/s)
ω_{max}	angular frequency of $\|Z_{max}\|$ (rad/s)
ω_{min}	angular frequency of $\|Z_{min}\|$ (rad/s)
ω_p	parallel resonance angular frequency, see Equation (1) (rad/s)
ω_s	series resonance angular frequency, $= (LC)^{-1/2}$ (rad/s)
Ω	$= (\omega/\omega_s)^2$
Ω_{max}	$= (\omega_{max}/\omega_s)2$
Ω_{min}	$= (\omega_{min}/\omega_s)^2$

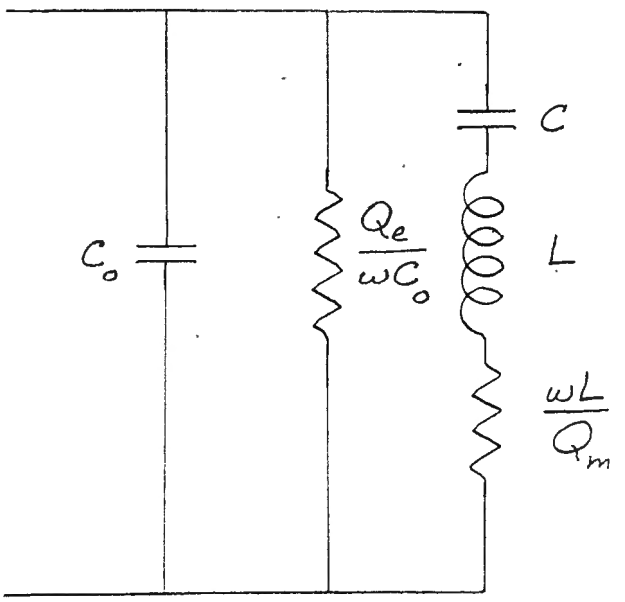

$$C = \frac{8}{\pi^2} k^2 C_o = \gamma C_o$$

$$L = (\omega_s^2 C)^{-1} = (\omega_s^2 \gamma C_o)^{-1}$$

$$k^2 << 1$$

Figure 1 - Simplified Equivalent Circuit of Half-Wavelength Piezoelectric Resonator with Electrical, as well as Mechanical, Losses

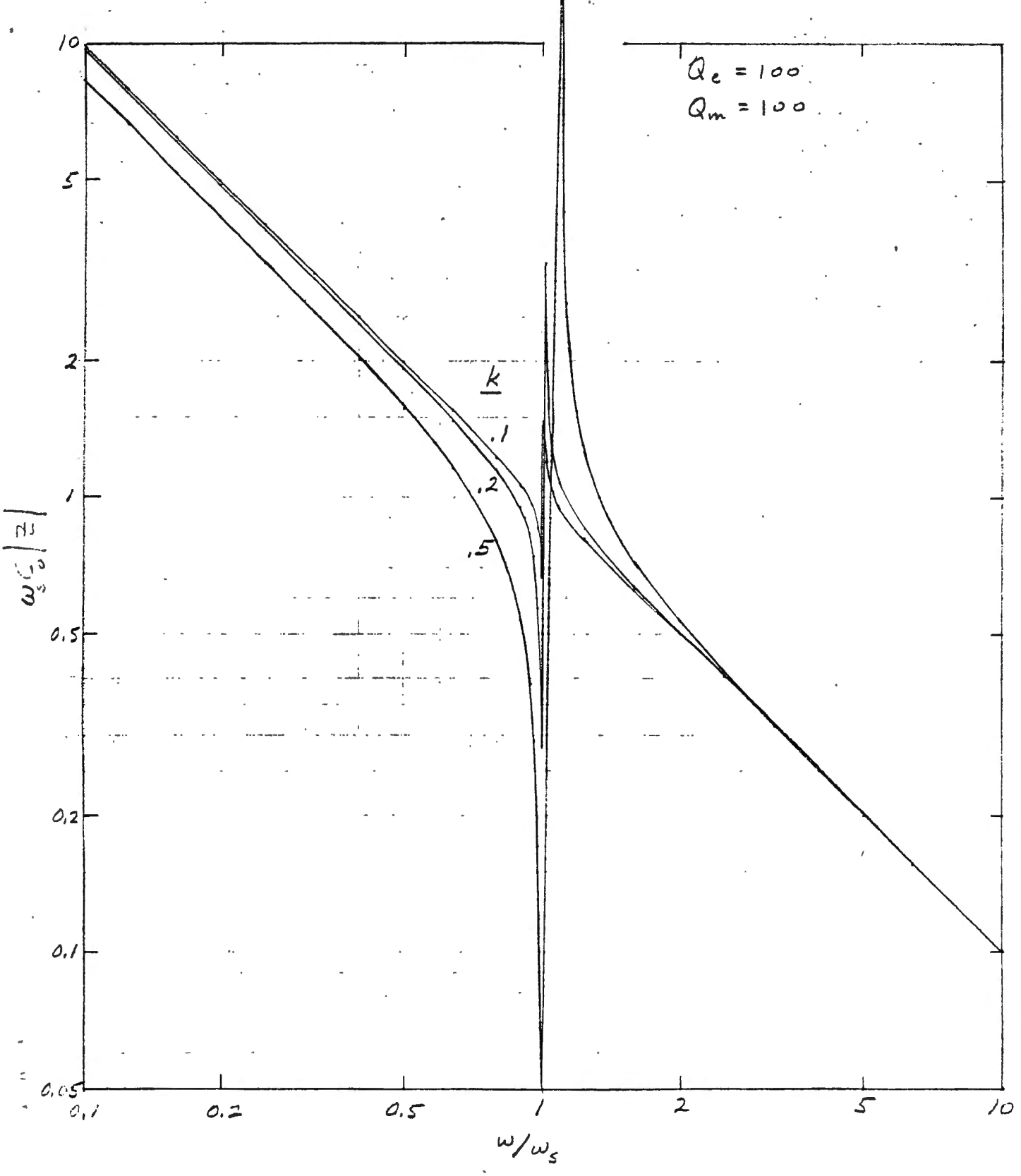

Figure 2 - Normalized Impedance Magnitude, Q_e=100, Q_m=100, k=0.1,0.2,0.5

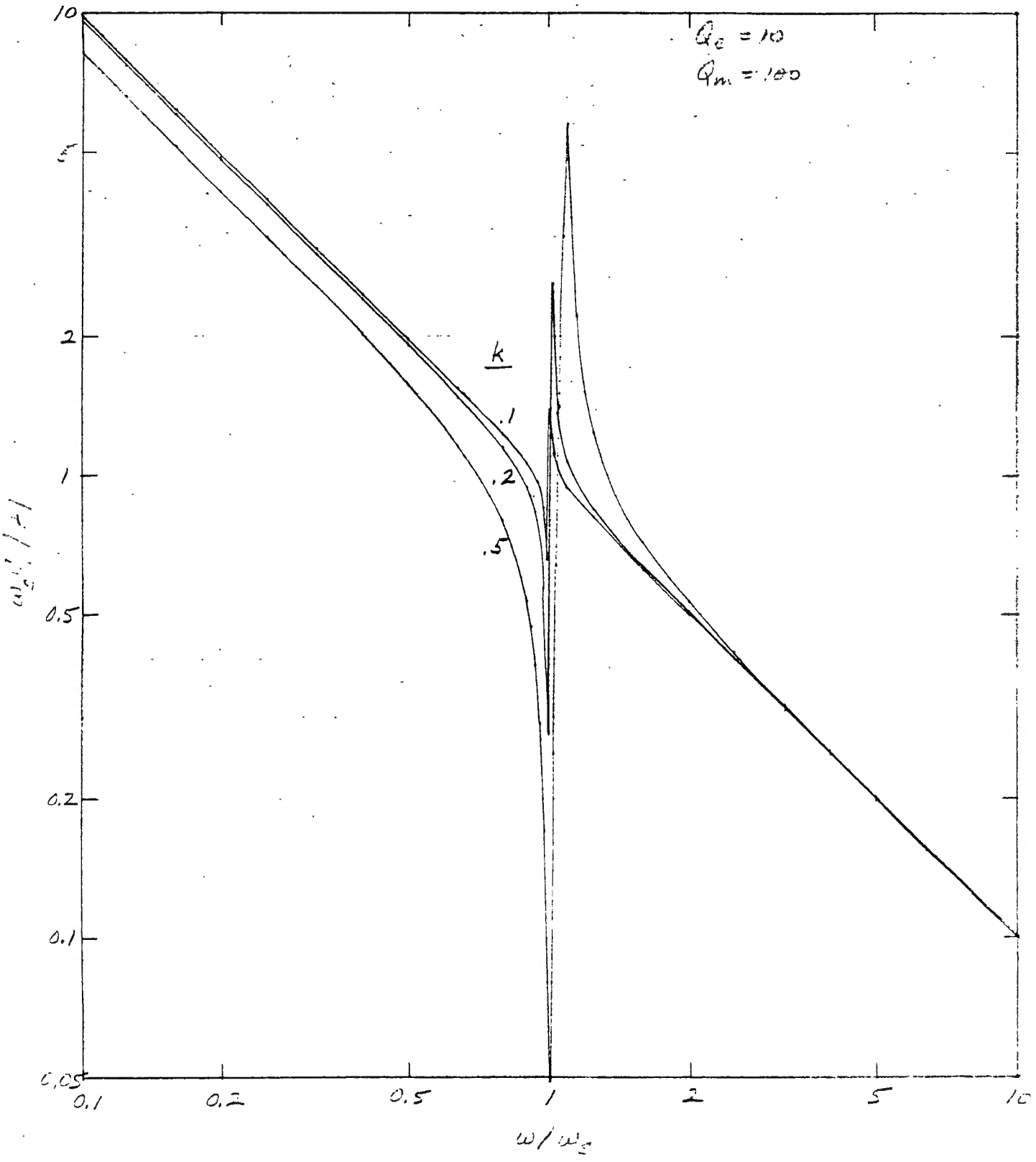

Figure 3 - Normalized Impedance Magnitude, Q_e=10, Q_m=100, k=0.1,0.2,0.5

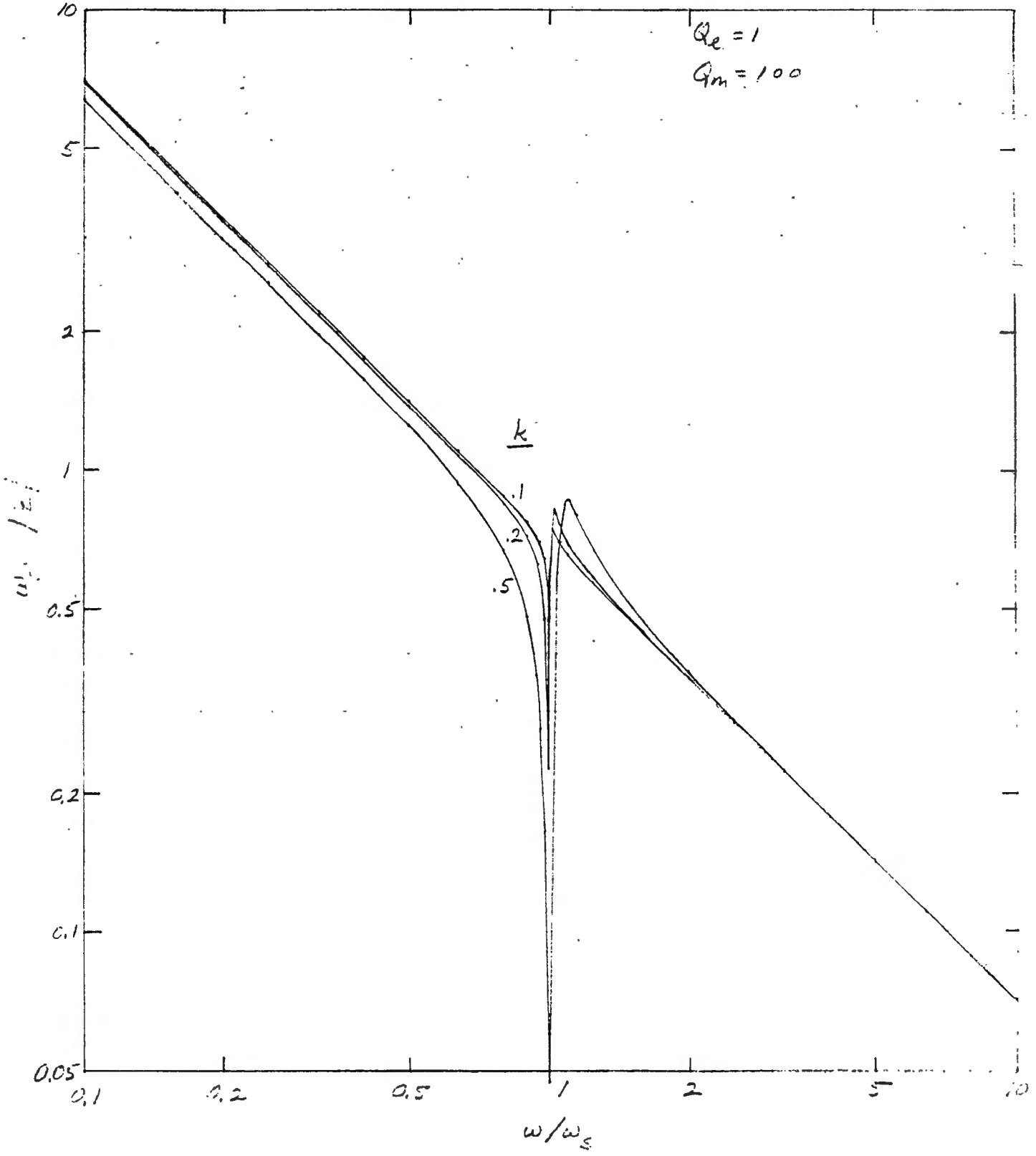

Figure 4 - Normalized Impedance Magnitude, Q_e=1, Q_m=100, k=0.1,0.2,0.5

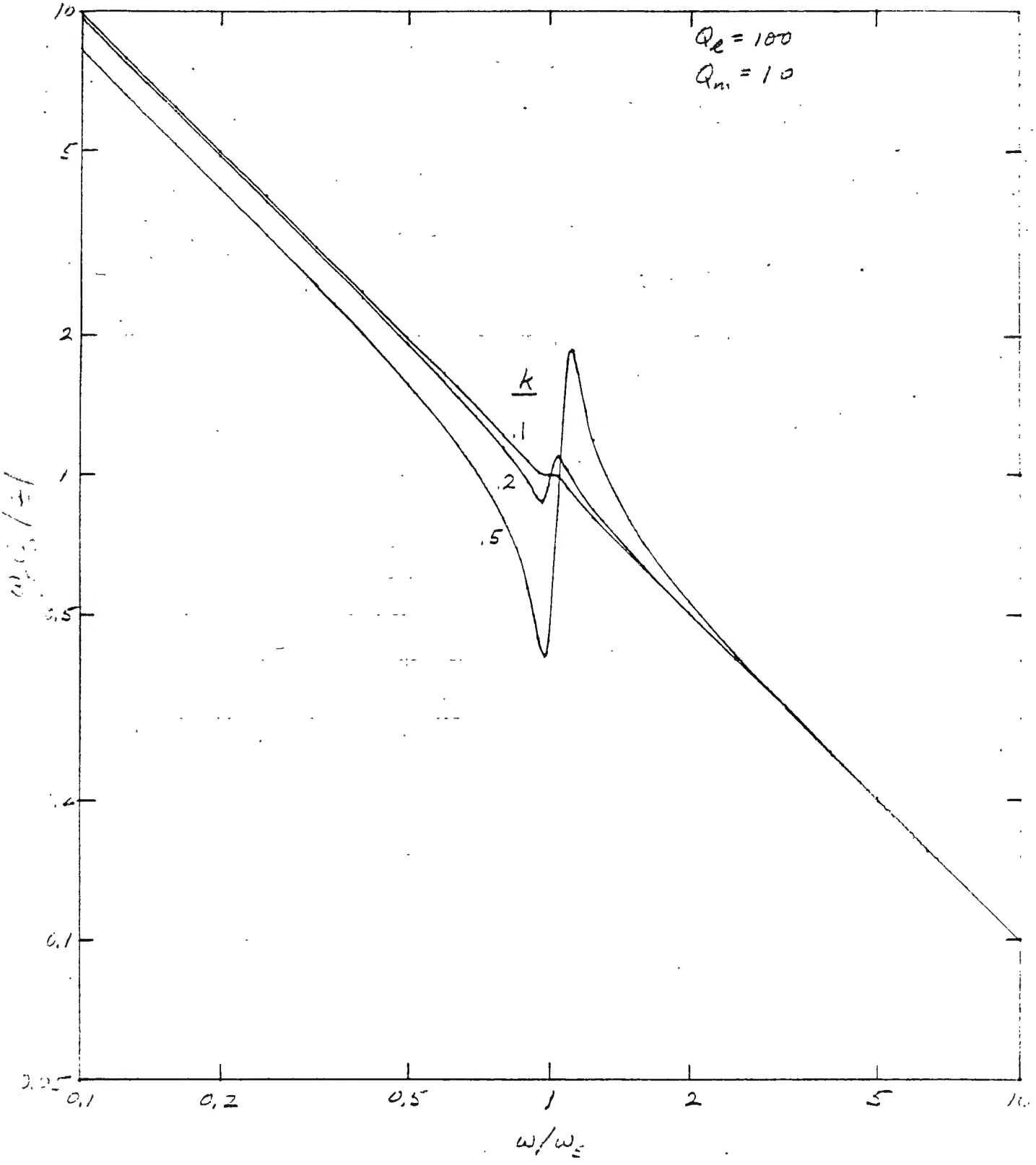

Figure 5 - Normalized Impedance Magnitude, Q_e=100, Q_m=10, k=0.1,0.2,0.5

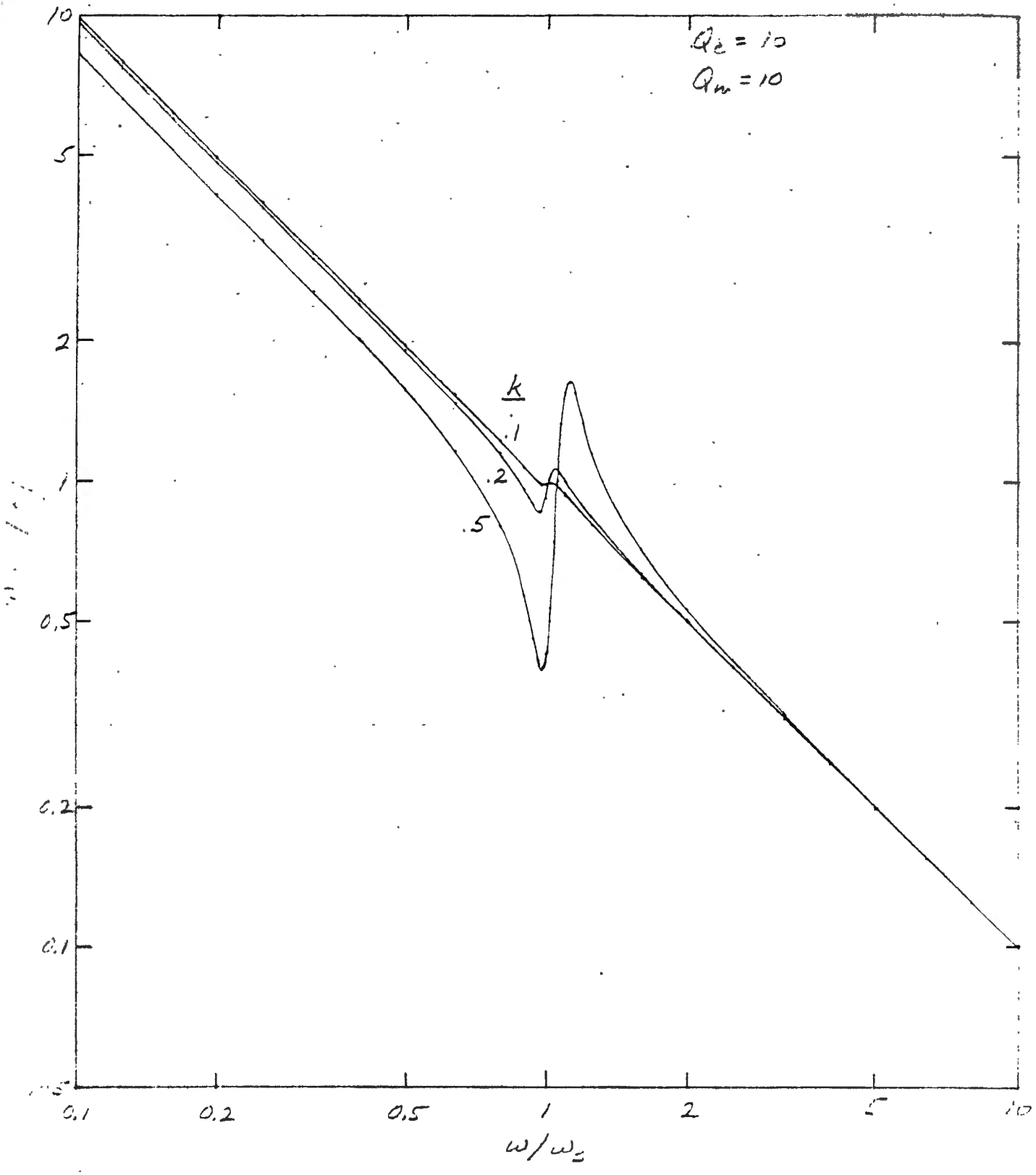

Figure 6 - Normalized Impedance Magnitude, Q_e=10, Q_m=10, k=0.1,0.2,0.5

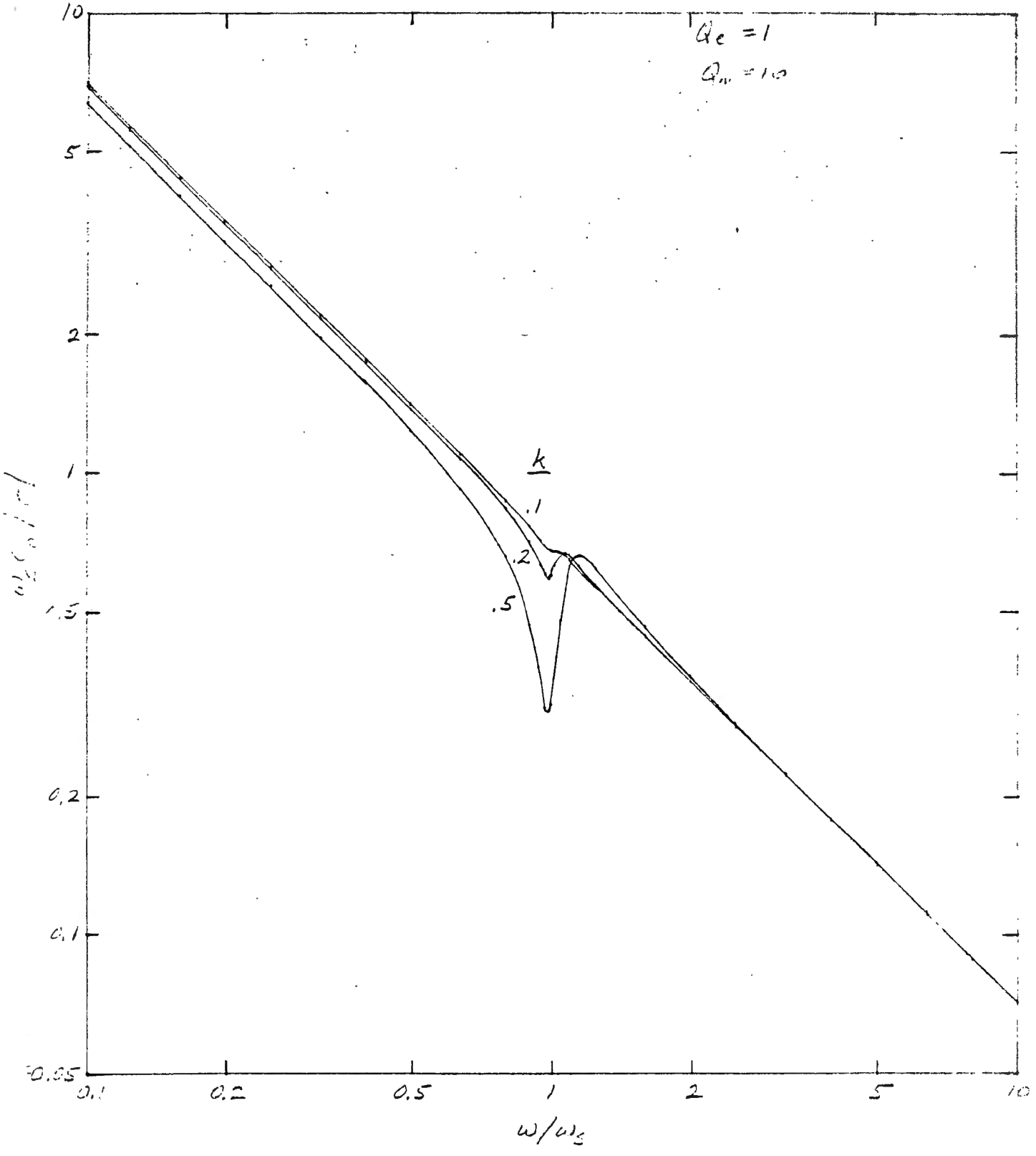

Figure 7 - Normalized Impedance Magnitude, Q_e=1, Q_m=10, k=0.1,0.2,0.5

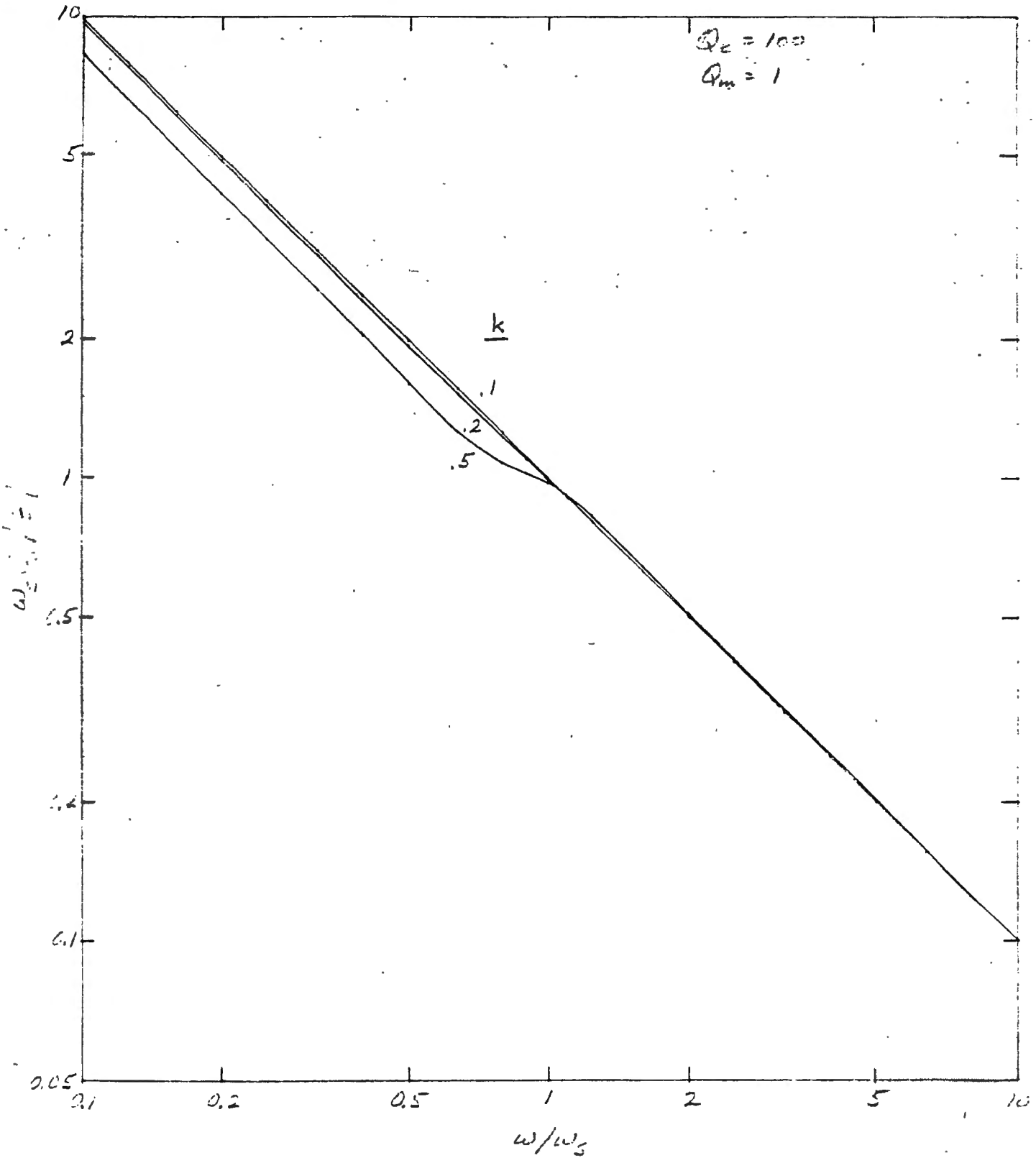

Figure 8 - Normalized Impedance Magnitude, Q_e=100, Q_m=1, k=0.1,0.2,0.5

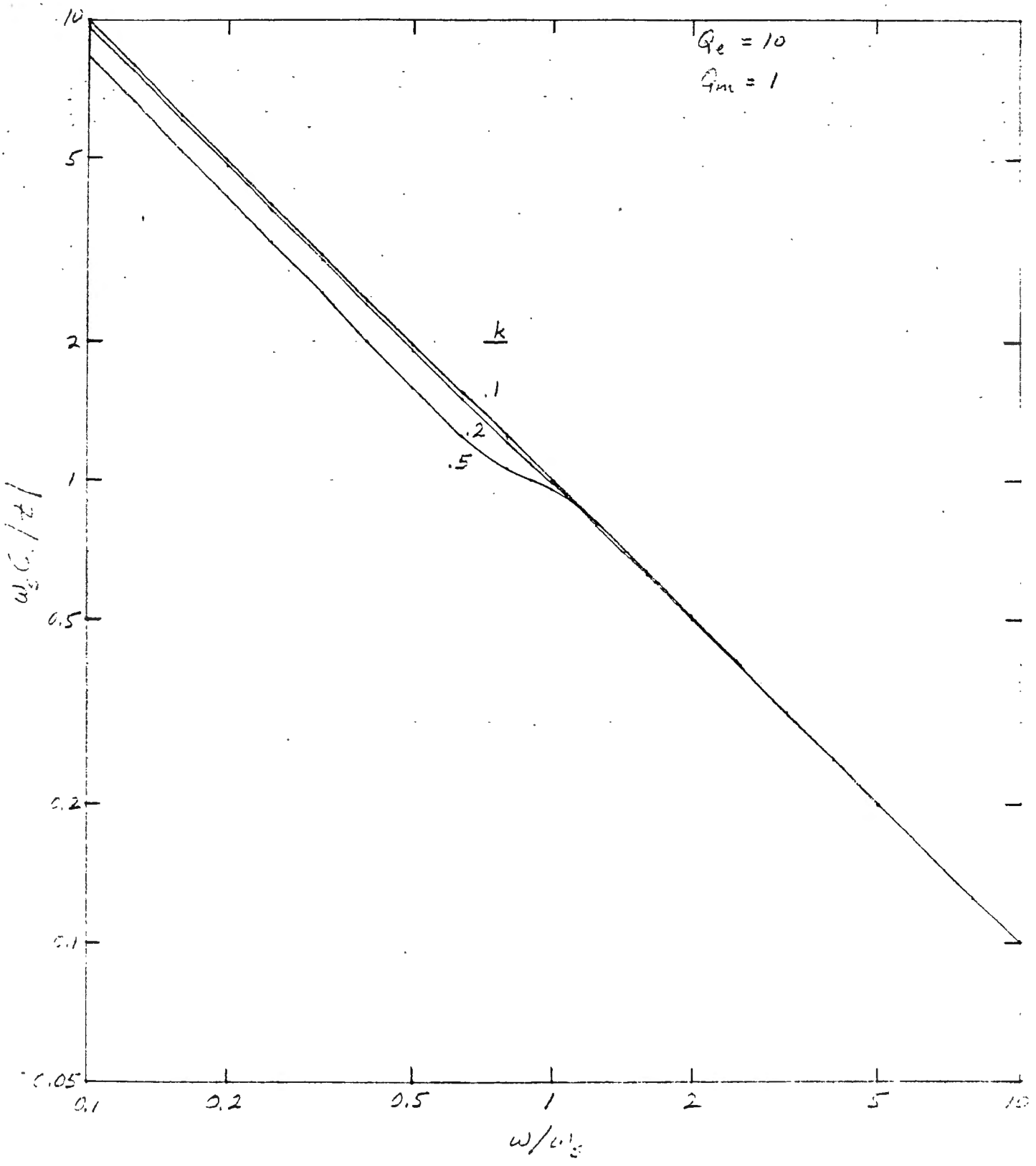

Figure 9 - Normalized Impedance Magnitude, Q_e=10, Q_m=1, k=0.1,0.2,0.5

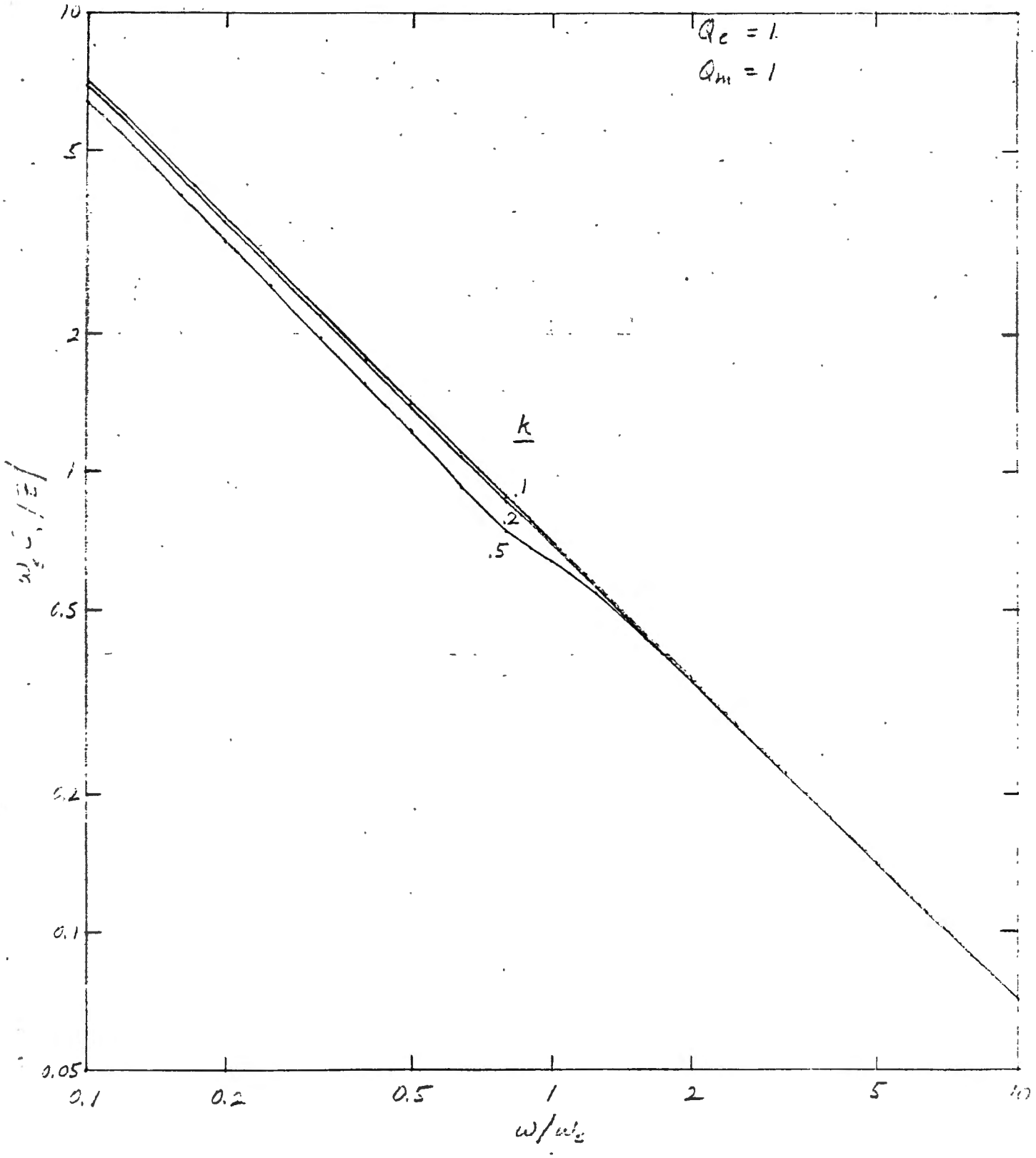

Figure 10 - Normalized Impedance Magnitude, Q_e=1, Q_m=1, k=0.1,0.2,0.5

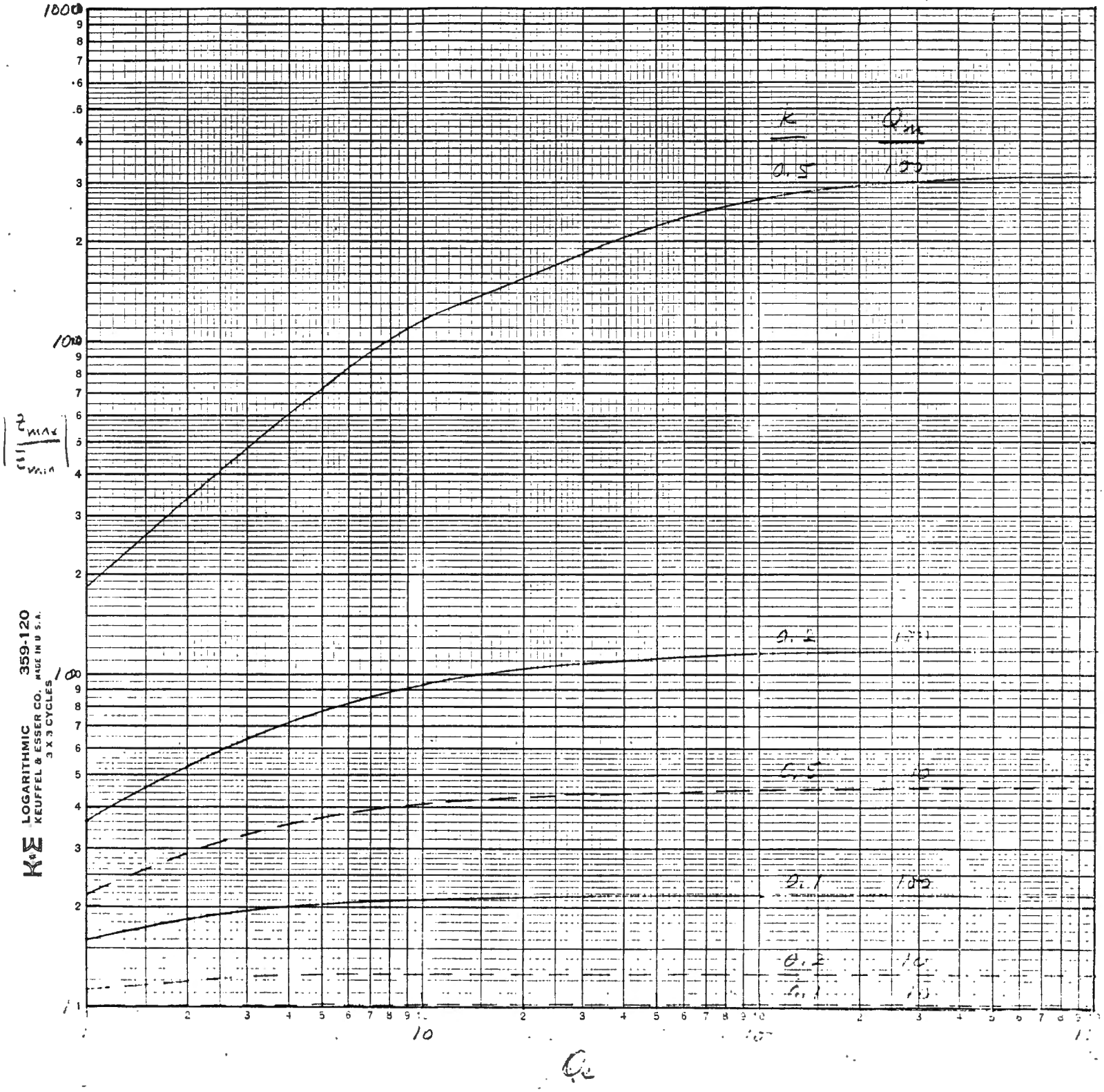

Figure 11 - Ratio of $|Z_{max}|$ to $|Z_{min}|$, k = 0.1, 0.2, 0.5. Solid Curves: Q_m = 100. Dashed Curves: Q_m = 10.

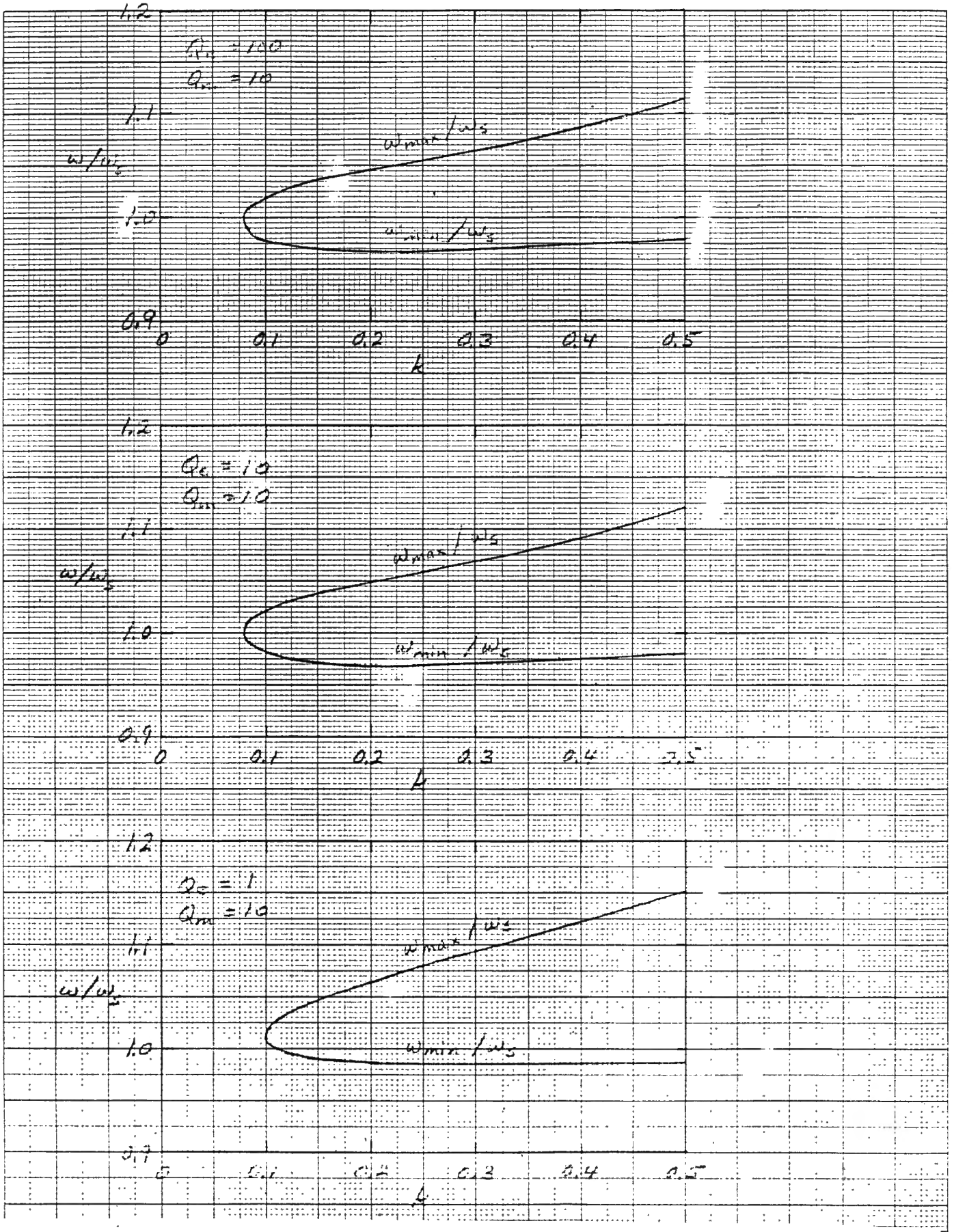

Figure 12 - Normalized Frequency of Maximum Impedance, ω_{max}/ω_s (upper branch), and of minimum impedance, ω_{min}/ω_s (lower branch), $Q_m = 10$, $Q_e = 100$, 10, 1.

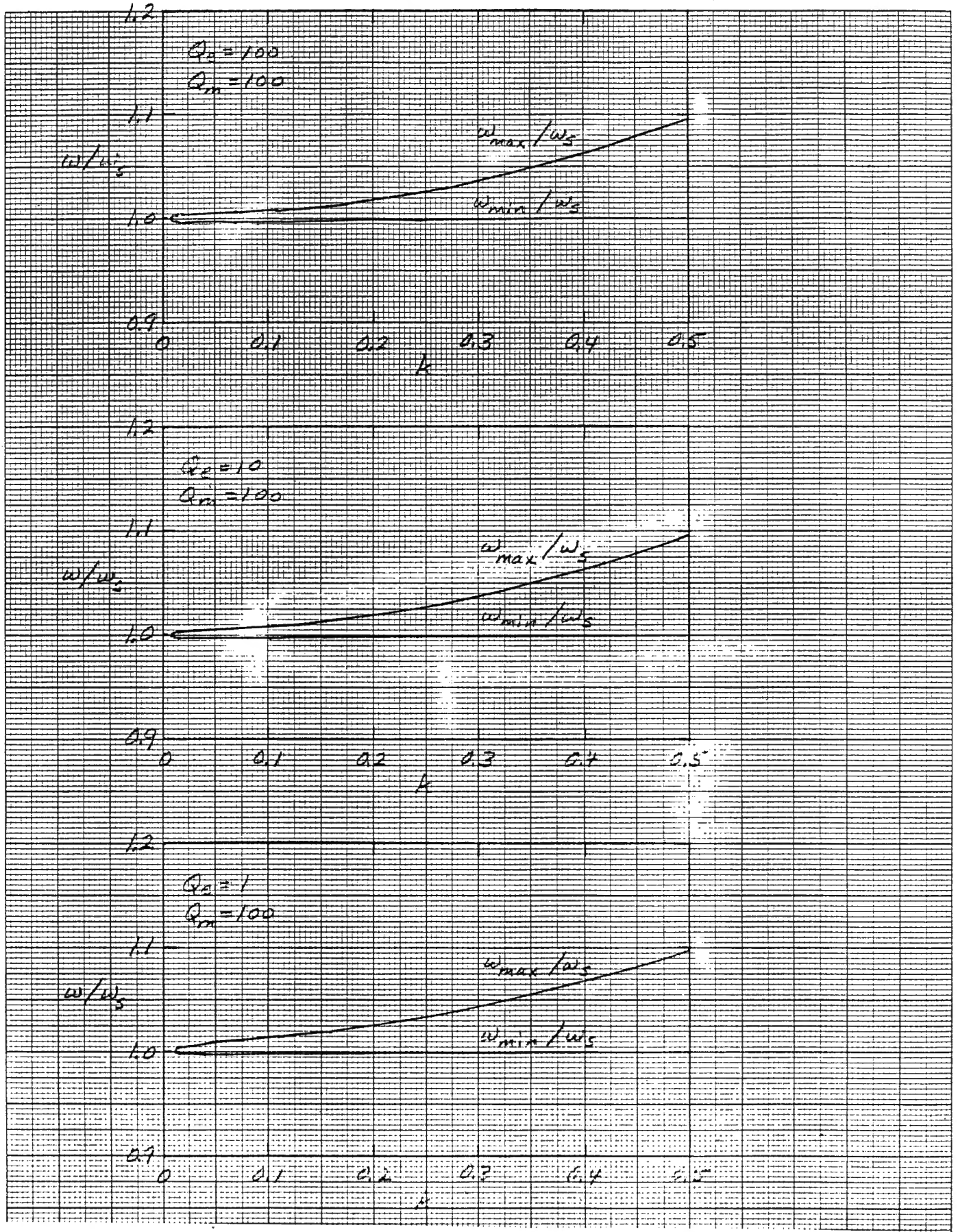

Figure 13 - Normalized Frequency of Maximum Impedance, ω_{max}/ω_s (upper branch), and of Minimum Impedance, ω_{min}/ω_s (lower branch), Q_m = 100, Q_e = 100, 10, 1.

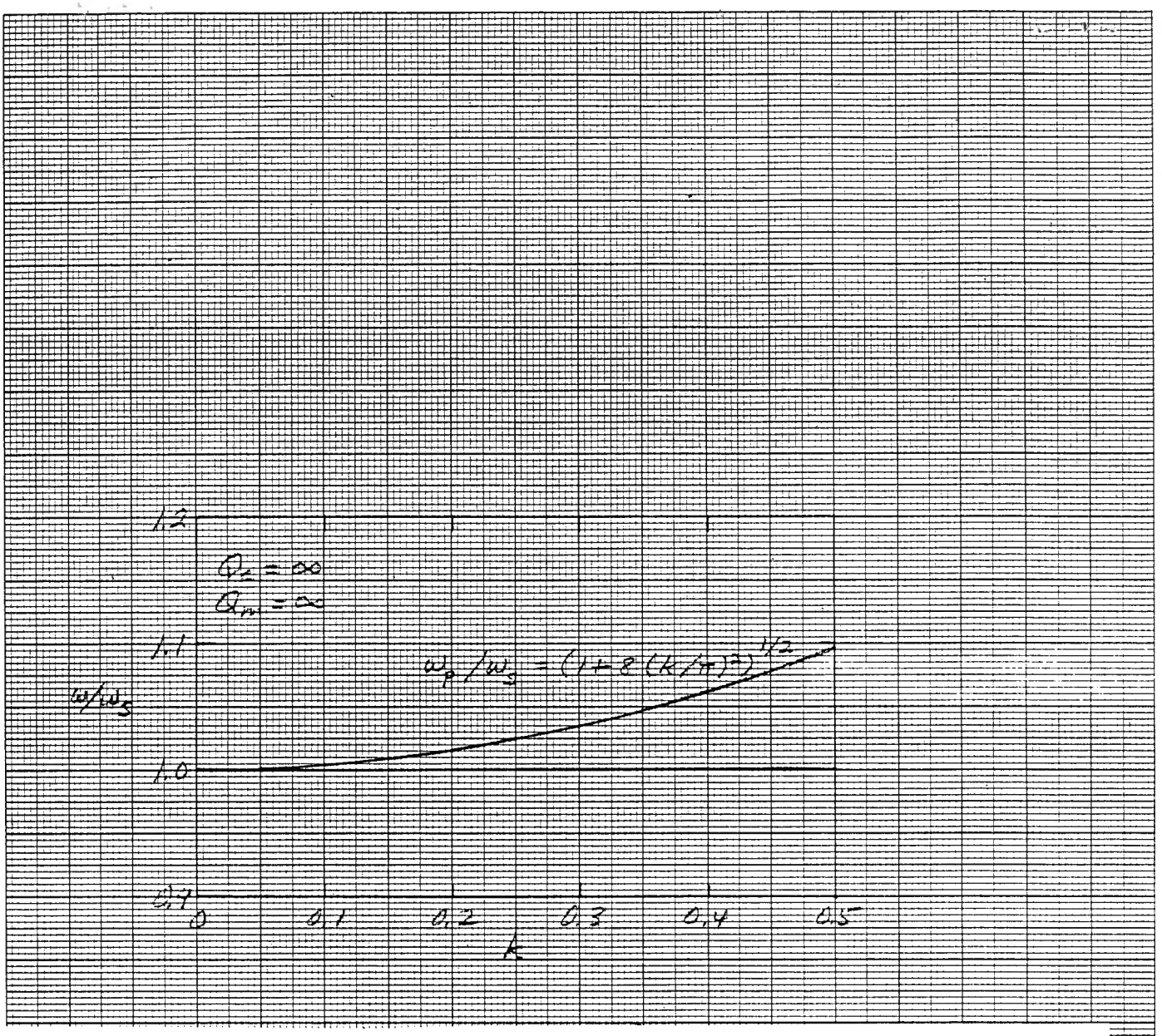

Figure 14 - Normalized Frequency of Infinite Impedance, ω_p/ω_s (upper branch), and of zero impedance, $\omega_s/\omega_s = 1$ (lower branch), $Q_m = Q_e = \infty$.

External
NAVSEA 63D
63R12 (C. C. Walker)
63X51 (C. A. Clark)
NOSC Code 712B (C. Hicks, J. Lockwood)
NRL/USRD (T. A. Henriquez, R. Y. Ting, A. L. Van Buren, J. Zalesak)
ONR Code 220 (CAPT E. Craig)
Code 2208 (T. Warfield)
Code 431 (R. C. Pohanka)
EDO Western Corp. (G. Snow)
General Dynamics, Electric Boat Division (E. Budzik)
Image Acoustics, Inc. (J. L. Butler)
Georgia Inst. of Tech. (J. Ginsberg, P. Rogers)
University of Leeds, England (I. M. Ward)
Martin Acoustics Software Technology (G. E. Martin)
Penn State University (L. E. Cross, R. E. Newnham)
Pennwalt Corp. (P. Bloomfield)
Physical Acoustics Corp. (J. Mitchell)
Raychem Corp. (G. Bischak, P. Soni)
Raytheon Corp. Research Div. (R. Tancrell)
Sub Signal Div. (S. Ehrlich, D. Ricketts)
ARL/UT (H. Frey, T. Muir)
Thorn EMI, Ltd. (D. M. Jones, J. C. McGrath)